NASA Technical Paper 2706

June 1987

On Minimizing the Number of Calculations in Design-by-Analysis Codes

Raymond L. Barger
and Anutosh Moitra

NASA

NASA
Technical
Paper
2706

1987

On Minimizing the Number of Calculations in Design-by-Analysis Codes

Raymond L. Barger
Langley Research Center
Hampton, Virginia

Anutosh Moitra
High Technology Corporation
Hampton, Virginia

National Aeronautics
and Space Administration

**Scientific and Technical
Information Office**

Summary

A method has been presented for aerodynamic design for a specified pressure distribution using analysis codes only. The method requires a very conservative number of analysis runs, and, therefore, is appropriate when the analysis code is a large code in terms of storage and/or running time. Three model problems illustrate some capabilities and limitations of the method.

Introduction

For some of the simpler aerodynamics design problems (especially two-dimensional), an inverse method exists so that a geometry can be directly generated from a specified pressure distribution. For somewhat more complex problems, an approximate inverse can be combined with an "exact" (in some sense) analysis code to yield, by iteration, a design to the accuracy of the analysis codes (refs. 1 and 2). For more complex problems, even an approximate inverse may not be available, or, if available, may be difficult to implement. Consequently, consideration has been given to design by the use of analysis codes only (refs. 3, 4, and 5). In this case, one approach is to treat the design problem as an optimization problem, with the objective function being the mean square error between the output pressure and the desired pressure.

Some problems inherent in the application of a numerical optimizer to such design problems have been discussed in some detail in references 4 and 5. The problem that is addressed here, however, is the one that arises when the analysis code is large in storage and/or running time. Then the many calculations required by a numerical optimizer to compute local sensitivities and gradually march toward the optimum become prohibitively lengthy and expensive. Furthermore, some problems incorporating inequality constraints can yield a design that represents a mathematical optimum but not an aerodynamically improved design. (See discussion in ref. 5.)

To avoid these problems, full advantage should be taken of such things as the designer's knowledge and experience, available experimental data, and previous calculations (refs. 4 and 5). One way that this information can be utilized is to generate a set of candidate shapes that are individually practical, although not optimal designs, so that an optimal combination of these shapes is obtained (ref. 3). This approach has at least two advantages. First, if the geometric constraints are linear and if each candidate shape satisfies the constraints, then a linear combination of the shapes satisfies the constraints. Therefore, the optimization procedure will not produce an aerodynamically impractical design. The second advantage to this approach is that, if each of the candidate shapes is a "good" shape (its performance is not too far from optimal), then presumably the optimizer has only a short distance to go to obtain the optimum; consequently, relatively few calculations are required.

These shape functions utilized by the optimizer are determined by a different process in the method of reference 5. There, they are selected to be "aerodynamically specific" so that one shape function is chosen to control airfoil thickness distribution, another to control camber distribution, etc. In the present procedure, the shapes utilized are all presumed to be intelligent guesses at an optimum design.

One way of representing the design problem is that of obtaining the maximum value for the negative of the mean square deviation of the obtained pressure distribution from the desired pressure distribution. With this characterization, the present method assumes that shape functions generated by the designer are rough approximations to the maximum, so that a sensitivity-type analysis can be applied locally near the maximum. In comparison, conventional optimizers only require that the initial guess functions lie somewhere on the "hillside" associated with the local maximum.

If the sensitivity analysis is valid near the optimum, and if the optimum geometry can be closely synthesized as a linear combination of the shape functions, then this optimum combination is generated by the analysis. Failure of either of these conditions is indicated by the results. In either case, additional shape functions must be added to the data base. These various situations are illustrated by the three model problems presented as examples.

The local sensitivity analysis near the maximum is analytical and uses the concept of base and calibration (or comparison) functions described in reference 6 and applied in references 7 and 8.

Symbols

$a, \tilde{a}, b, c$	coefficients used in various series of developments
C_p	pressure coefficient
d	difference function, $p_d - p$ (see eqs. (5))
d_r	$= p_d - p_b$ (see eqs. (5))
$\tilde{e}_i$	mutually orthogonal functions
e_i	mutually orthonormal functions
E	error function (eq. (8))
(F_1, F_2)	inner product of functions F_1 and F_2, defined by equation (A1)

f	function denoting input to computer program
L	linear operator defined by equation (1)
M	free-stream Mach number
p	static pressure distribution
p_∞	free-stream pressure
$Q[f]$	nonlinear operator symbolically denoting output of analysis code
r	radial coordinate
x, y, z	Cartesian coordinates
$\tilde{y}$	value of y normalized with respect to edge value
α	incidence angle

Subscripts:

b	base function
d	desired, or design, pressure distribution
n	denotes quantity in nth term of series

Analysis

As in reference 8, the analysis code, or system of codes, is treated as an operator operating on the input function. Furthermore, the linearity assumption for input increments is made. This assumption, which is the basis for sensitivity analysis, requires that the variations in the output of the program be approximately linear functions of the corresponding small increments in the input function. When this condition is not met, as, for example, in problems involving shock waves, the problem can sometimes be preconditioned so that it becomes linear in small variations. Such a preconditioning technique by coordinate stretching is described in reference 7.

The linearity condition can be expressed symbolically (as in ref. 8). Let f denote the input function and let $Q[f]$ denote symbolically the nonlinear operator represented by the computer code. Then, it is assumed that Q behaves as a (Gateaux) differentiable operator, so that, for increments δf in f, the variation in the operator is approximately represented by its first variation, L, which is linear in δf. In equation form,

$$Q[f_o + \delta f] - Q[f_o] = L[\delta f] \tag{1}$$

In other words, for slightly different input functions f_o and $f_o + \delta f$, the difference in the output is linear in δf.

The method to be described is fairly general in concept. However, for purposes of simplicity in presentation it will be discussed in terms of a typical problem—that of designing a geometry to obtain a close approximation to a desired pressure distribution.

Assume then that several configurations, represented by the inputs f_i $(i = 1, \ldots, n)$ have been analyzed so that the corresponding output pressure distributions p_i are available. It is assumed that the f_i functions are aerofunction shapes (in the sense of ref. 4), that each f_i satisfies the required geometric constraints, and that each f_i has been initially selected so that the corresponding p_i roughly approximates the desired pressure distribution p_d.

One might attempt to represent the desired distribution p_d as a linear combination of the p_i,

$$p_d \approx \sum_1^n \tilde{a}_i p_i \tag{2}$$

However, some constraint is normally applied to the $\tilde{a}_i$ as a result of geometric constraints on the input geometries. The most natural constraint, as is shown later, is to require

$$\sum_1^n \tilde{a}_i = 1 \tag{3}$$

This constraint reduces the number of arbitrary coefficients in equation (2) to $n-1$. Thus, a new set of $n-1$ coefficients a_i $(i = 1, \ldots, n-1)$ is defined by

$$p_d - p_n \approx \sum_1^{n-1} a_i (p_n - p_i) \tag{4a}$$

This equation can also be written in the form

$$p_d \approx p_n + \sum_1^{n-1} a_i (p_n - p_i) \tag{4b}$$

or

$$p_d = \left(1 + \sum_1^{n-1} a_i\right) p_n - \sum_1^{n-1} a_i p_i \tag{4c}$$

Comparing equation (4c) with equation (2) yields the relation between the a_i and $\tilde{a}_i$ coefficients. (See eq. (15).) In the form of equation (4c), it is clear that the coefficients sum to one.

In equation (4a), p_n is denoted the base function and the remaining p_i values are the calibration, or comparison, functions. Actually, any one of the computed p_i can be selected as the base function and

the remaining functions renumbered from 1 to $n-1$. Thus, for the representation

$$p_d - p_b \approx \sum_1^{n-1} a_i (p_b - p_i) \tag{5a}$$

or with the difference notation

$$d_r \approx \sum_1^{n-1} a_i d_i \tag{5b}$$

the problem is to determine the a_i so that the right-hand side is the closest possible approximation to the left-hand side. If the representation functions d_i were orthogonal, the a_i would be determined by the Fourier coefficient formulas in order to yield the minimum square error. In general, these functions are not orthogonal, but they can be orthogonalized and normalized by the well-known Gram-Schmidt procedure (ref. 9, p. 116, for example). That is, a set of orthonormal functions e_i ($i = 1, \ldots, n-1$) can be determined as linear combinations of the d_i:

$$e_i = \sum_{j=1}^{i} c_{ij} d_j \tag{6}$$

The details of calculating the c_{ij} by the Gram-Schmidt method are straightforward but rather lengthy and therefore are relegated to the appendix.

Now d_r is approximated by a linear combination of the orthonormal functions

$$d_r \approx \sum_1^{n-1} b_i e_i \tag{7}$$

Then, the coefficients b_i are determined by the Fourier formula in order to obtain the best approximation, in the mean square sense, to d_r. That is, with the terminology defined by equations (A1) and (A2) for the error function

$$E \equiv d_r - \sum_1^{n-1} b_i e_i \tag{8}$$

the quantity $|E|$ is minimized when the b_i coefficients are obtained from the formulas

$$b_i = (d_r, e_i) \tag{9}$$

To be useful, the approximation in equation (7) must be expressed in terms of the original differences d_i; this is accomplished by using equation (6):

$$\begin{aligned}
\sum_1^{n-1} b_i e_i &= \sum_{i=1}^{n-1} b_i \sum_{k=1}^{i} c_{ik} d_k \\
&= \sum_{i=1}^{n-1} b_i \sum_{k=1}^{n-1} c_{ik} d_k \qquad (c_{ik} = 0 \text{ for } k > i) \\
&= \sum_{k=1}^{n-1} \left(\sum_{i=1}^{n-1} b_i c_{ik} \right) d_k \qquad (c_{ik} = 0 \text{ for } k > i) \\
&= \sum_{k=1}^{n-1} a_k d_k
\end{aligned} \tag{10a}$$

with

$$a_k = \sum_{i=1}^{k} b_i c_{ik} \tag{10b}$$

Now, replacing the differences in equation (7) with the pressure functions (eqs. (5b) and (5c)) and substituting from equations (10) into the result yield

$$p_d - p_b \approx \sum_1^{n-1} a_k (p_k - p_k) \tag{11}$$

with a_k given by equation (10b). If the pressures in equation (11) are written as operators operating on the shape functions, it has the form

$$Q(f_d) - Q(f_b) \approx \sum_1^{n-1} a_k [Q(f_b) - Q(f_k)] \tag{12a}$$

Applying the linearity assumption (eq. (1)) yields

$$\begin{aligned}
L(f_d - f_b) &\approx \sum_1^{n-1} a_k L(f_b - f_k) \\
&= L\left[\sum_1^{n-1} a_k (f_b - f_k) \right]
\end{aligned} \tag{12b}$$

If it is assumed that, locally, L is uniquely invertible then

$$f_d - f_b \approx \sum_1^{n-1} a_k (f_b - f_k) \tag{13a}$$

or

$$f_d = \left(1 + \sum_1^{n-1} a_k \right) f_b - \sum_1^{n-1} a_k f_k \tag{13b}$$

Equation (13b) can also be written as

$$f_d \approx \sum_1^{n} \tilde{a}_k f_k \tag{14}$$

where

$$\tilde{a}_k = \left\{ \begin{array}{ll} -a_k & (k = 1, \ldots, n-1) \\ 1 + \sum_{1}^{n-1} a_k & (k = n) \end{array} \right\} \quad (15)$$

Equations (14) and (15) yield the optimum combination of the shapes f_i, $i = 1, \ldots, n$ subject to the constraint of equation (3). The significance of this constraint is now apparent. It constrains the overall size of the combination shape

$$\sum_{1}^{n} \tilde{a}_k f_k$$

If, for example, the shapes were axisymmetric forebody shapes with a fixed base radius, the optimum combination would also have the required base radius. Similarly, if the slope at the nose were constrained to have a fixed value so that each f_k had this required slope, then the optimum combination would have the required slope. Such constraints, though basic, are nonlinear, and so are not automatically satisfied by a linear combination of shapes that individually satisfy the constraints. Hence, the requirement for equation (3).

Equations (14) and (15) give the optimum combination of the original shapes—a shape that will yield the closest approximation to the desired pressure distribution subject to the constraint of equation (3) and within the accuracy of the sensitivity analysis assumption of local linearity. A computer program that calculates the coefficients $\tilde{a}_k$ requires, at most, a few seconds running time on a modern computer. In comparison, the analysis program that computes the pressures may require minutes to perhaps hours if, for example, a Navier-Stokes code is used.

After the pressure has been calculated for the optimum combination a better approximation can be obtained by adding new geometries to the data base. The relative values of the coefficients defining the optimum combination shape should provide some insight as to the manner in which the geometry should be varied in order to improve the approximation.

The mathematics of this derivation is exact. The extent to which the optimal shape derived actually approximates the desired result depends primarily on two factors. The first of these is the extent to which the original data base provides the types of shapes that are effective in approximating the required result, subject to the applied constraints. The influence of this factor is seen in the results obtained for the second model problem discussed in the following section.

The second factor depends on the accuracy of the local linearity assumption. If the difference functions involved in the derivation of the coefficients do not have small amplitudes, the linearity condition is violated. Local nonlinearity may also be associated with the manner in which constraints are (or are not) applied. The influence of this factor is seen in the results obtained for the first model problem discussed in the following section.

Results on Model Problems

Three model problems were selected to illustrate the application of the theory. The calculations involved are much simpler than the type of complex calculation for which the method was intended. However, simplicity in model problems permits one to concentrate on fundamental concepts without lengthy explanation of extraneous considerations. Thus, although the power of the technique is not adequately demonstrated, the problems selected are sufficient to illustrate the application of the method, its accuracy, and some problems that can arise.

The first problem is that of designing a body for a specified upper-surface spanwise pressure distribution as a function of cross-section shape. The design conditions were $M = 1.4, \alpha = 5°$, body planform described by the equation $y = 0.5 \times (1 - x)$, Length = 10 units, pressure specified at $x = 7.5$, and body semi-height to span ratio at $x = 7.5$ is 1/3. Each of four data base calculations satisfied these conditions, but with cross-section shapes specified by the equations

$$z_1(\tilde{y}) = \frac{1}{6}\left(1 + \sqrt{1 - \tilde{y}^2} - 2\tilde{y}^2 + \tilde{y}^3\right)$$

$$z_2(\tilde{y}) = \frac{1}{3}\sqrt{1 - \tilde{y}^2}$$

$$z_3(\tilde{y}) = \frac{1}{6}\left(2\sqrt{1 - \tilde{y}^2} - \tilde{y}^2 + \tilde{y}^3\right)$$

$$z_4(\tilde{y}) = \frac{1}{3}\left(-2 + 3\sqrt{1 - \tilde{y}^2} - \tilde{y}^2 + 3\tilde{y}^3\right)$$

where $\tilde{y}$ is the y coordinate normalized with respect to its edge value. They are shown in figure 1(a). The pressures were computed by using the finite-volume Euler code described in reference 10. Figure 1(b) shows the design pressure distribution that was specified and the pressure distributed for the four base shapes. Figure 1(c) shows the design pressure distribution, the theoretically predicted best approximation that can be obtained with the four available results (from eq. (2)), as well as the actual result obtained by computing the pressure for the optimum combination shape. This cross-section shape is also

shown in figure 1(c). Figure 1(d) compares the design distribution with that obtained for the optimum combination and with the closest approximation obtained with a single data base shape.

The only geometric constraint that was applied explicitly to the cross-section shape was the requirement that the body semi-height be 1/3 the span at $x = 7.5$. Since each of the data base shapes satisfies this condition, the optimum combination shape also satisfies the condition.

However, no geometric constraint was applied at the cross-section edge. The four data base shapes represent a considerable range of edge curvatures. This factor contributes to the considerable nonlinearity occurring in the calculations, as is demonstrated by the significant difference between the actual and predicted pressures for the combination shape. The edge represents the leading edge for the crossflow, and, consequently, its curvature has a dominating effect on the spanwise pressure distribution. In fact, if the optimal shape had a relatively small edge radius, a crossflow shock would be generated; in which case, the linearity would be completely destroyed. A small edge radius would also present the problem of upper surface separation. The shapes analyzed avoid this problem but just marginally, a factor that may also contribute to the nonlinearity. However, even with the error that results from the nonlinearity, the calculation provides useful information, and the resulting pressure distribution represents an improved approximation to the specified distribution. The shape generated could now be used as a base shape with new comparison functions generated as small perturbations of this shape.

The second model problem was to design a body of revolution for a low-speed pressure distribution specified at $\alpha = 0°$ over the forward 60 percent of the body. Four shapes, shown in figure 2(a) were analyzed by a panel method (ref. 11), with the pressure distribution for each data base body shape shown in figure 2(b). The design pressure distribution (fig. 2(c)) was specified up to the 70-percent station only, with the anticipation that a smooth fairing beyond the 70-percent station would not significantly affect the pressures up to the 60-percent station.

The predicted and computed pressure distributions for the optimal combination are also shown in figure 2(c), along with the optimal shape. It is seen that the predicted distribution corresponds fairly closely with the computed distribution up to the 60-percent station. The difference between the specified pressure and the predicted pressure results from the failure of the data base shapes to provide sufficient variation in their corresponding pressure distributions. This difference could be decreased by judiciously adding to the data base.

The third model problem studied was to design an axisymmetric supersonic forebody for a specified meridian pressure distribution at $M = 3.0$. Geometric constraints were Length-to-diameter ratio = 2.5, Semicone angle nose = 16.7°, and zero slope at base ($x = 1.0$). Four configurations were analyzed, with shapes described by the equations

$$r_1(x) = 0.3x - 0.1x^3 \qquad (0 \le x \le 1)$$
$$r_2(x) = r_1(x) + 0.04(sin\,\pi x)^2$$
$$r_3(x) = r_1(x) + 0.1x^3(1-x)^2$$
$$r_4(x) = r_1(x) + 0.1x^2(1-x)^3$$

The corresponding pressure distributions, computed by the method of reference 12 are shown in figure 3(a). The specified design pressure distribution and the predicted and computed pressure distributions are all shown in figure 3(b), as well as the corresponding body shape.

Although each of the distributions in figure 3(a) falls generally above the specified design distribution, the result for the optimum combination matches the required distribution closely.

Furthermore, the fact that the predicted result closely approximates the computed result for the optimum combination indicates that the problem, as formulated, has a high degree of linearity. This results from the closely controlled end constraints as well as the basic nature of the problem.

Concluding Remarks

A method has been presented for aerodynamic design using an analysis code only. The method is appropriate when the analysis code is a large code in terms of storage and/or running time so that minimizing the number of analysis runs is crucial. The designer is required to furnish several intelligently selected shape functions whose performances represent rough approximations to the optimum. Then the method yields the optimum combination of the shape functions. This combination is a close approximation to the actual optimum provided that (1) the original shape functions were sufficiently close to the optimum and (2) there is sufficient variety in the corresponding pressure distributions so that the desired distribution can be closely represented as a linear combination of the base distributions. Three model problems were presented to illustrate the salient features of the method.

NASA Langley Research Center
Hampton, VA 23665-5225
April 28, 1987

Appendix

Gram-Schmidt Orthogonalization and Series Expansion of Difference Functions

The inner product of two functions d_i and d_j is defined by the equation

$$(d_i, d_j) = \int d_i(x)\, d_j(x)\, dx \tag{A1}$$

where the integral is evaluated over the relevant domain. The corresponding norm is

$$|d_i| = \sqrt{(d_i, d_i)} \tag{A2}$$

Then, the orthonormal set e_i is defined recursively by the following procedure:

$$e_1 = \frac{d_1}{|d_1|} \tag{A3}$$

$$\tilde{e}_2 = d_2 - (d_2, e_1)\, e_1 \tag{A4a}$$

$$e_2 = \frac{\tilde{e}_2}{|\tilde{e}_2|} \tag{A4b}$$

$$\tilde{e}_i = d_i - \sum_{j=1}^{i-1} (d_i, e_j)\, e_j \tag{A5a}$$

$$e_i = \frac{\tilde{e}_i}{|\tilde{e}_i|} \tag{A5b}$$

This procedure is sufficient to derive the e_i functions from the d_i functions. However, it is advantageous to express the e_i as linear combinations of d_i:

$$e_i = \sum_{j=1}^{i} c_{ij} d_j \tag{A6}$$

The coefficients in equation (A6) are computed as follows. From equation (A3),

$$c_{11} = \frac{1}{|d_1|}$$

From equations (A4),

$$c_{22} = \frac{1}{|\tilde{e}_2|}$$

$$c_{21} = \frac{(d_2, e_1)}{|\tilde{e}_2||d_1|}$$

For the general term, we substitute into the summation in equation (A5a) from equation (A6):

$$\begin{aligned}
\tilde{e}_i &= d_i - \sum_{j=1}^{i-1} (d_{ij}, e_j) \sum_{k=1}^{j} c_{jk} d_k \\
&= d_i - \sum_{j=1}^{i-1} (d_{ij}, e_j) \sum_{k=1}^{i-1} c_{jk} d_k \qquad (c_{jk} = 0 \text{ for } k > j) \\
&= d_i - \sum_{k=1}^{i-1} \sum_{j=1}^{i-1} (d_i, e_j)\, c_{jk} d_k \qquad (c_{jk} = 0 \text{ for } k > j) \\
&= d_i - \sum_{k=1}^{i-1} \tilde{c}_{i-1,k} d_k
\end{aligned} \tag{A7}$$

where

$$\tilde{c}_{i-1,k} = \sum_{j=1}^{i-1} (d_i, e_j)\, c_{jk} \qquad (c_{jk} = 0 \text{ for } k > j) \tag{A8}$$

Finally, using equations (A7) and (A8) with equation (A5b) in equation (A6) yields

$$c_{ik} = \left\{ \begin{array}{ll} \frac{1}{|\tilde{e}_i|} & (k = i) \\ \frac{\tilde{c}_{ik}}{|\tilde{e}_i|} & (k < i) \end{array} \right\} \tag{A9}$$

where the coefficients $\tilde{c}_{ik}$ are obtained recursively from equation (A8). Thus, with c_{ik} computed by relation (A9), equation (A6) is the result required in the main text (eq. (6)).

References

1. Barger, Raymond L.; and Brooks, Cuyler, W., Jr.: *A Streamline Curvature Method for Design of Supercritical and Subcritical Airfoils.* NASA TN D-7770, 1974.
2. Davis, Warren H., Jr.: Technique for Developing Design Tools From the Analysis Methods of Computational Aerodynamics. *AIAA J.*, vol. 18, no. 9, Sept. 1980, pp. 1080–1087.
3. Vanderplaats, Garret N.: An Efficient Algorithm for Numerical Airfoil Optimization. AIAA-79-0079, Jan. 1979.
4. Aidala, P. V.; Davis, W. H., Jr.; and Mason, W. H.: Smart Aerodynamic Optimization. AIAA-83-1863, July 1983.
5. Davis, W. H., Jr.: TRO-2D: A Code for Rational Transonic Aerodynamic Optimization. AIAA-85-0425, Jan. 1985.
6. Stahara, S. S.; Crisalli, A. J.; and Spreiter, J. R.: Evaluation of a Strained-Coordinate Perturbation Procedure: Nonlinear Subsonic and Transonic Flows. AIAA-80-0339, Jan. 1980.
7. Nixon, David: Perturbation of a Discontinuous Transonic Flow. *AIAA J.*, vol. 16, no. 1, Jan. 1978, pp. 47–52.
8. Barger, Raymond L.: *Solution of Complex Nonlinear Problems by a Generalized Application of the Method of Base and Comparison Solutions With Applications to Aerodynamics Problems.* NASA TP-1857, 1981.
9. Taylor, Angus E.: *Introduction to Functional Analysis.* John Wiley & Sons, Inc., c.1958.
10. Moitra, Anutosh: Euler Solutions for High-Speed Flow About Complex Three-Dimensional Configurations. AIAA-86-0246, Jan. 1986.
11. Maskew, Brian: Prediction of Subsonic Aerodynamic Characteristics: A Case for Low-Order Panel Methods. *J. Aircr.*, vol. 19, no. 2, Feb. 1982, pp. 157–163.
12. Marconi, Frank; and Yeager, Larry: *Development of a Computer Code for Calculating the Steady Super/Hypersonic Inviscid Flow Around Real Configurations. Volume II—Code Description.* NASA CR-2676, 1976.

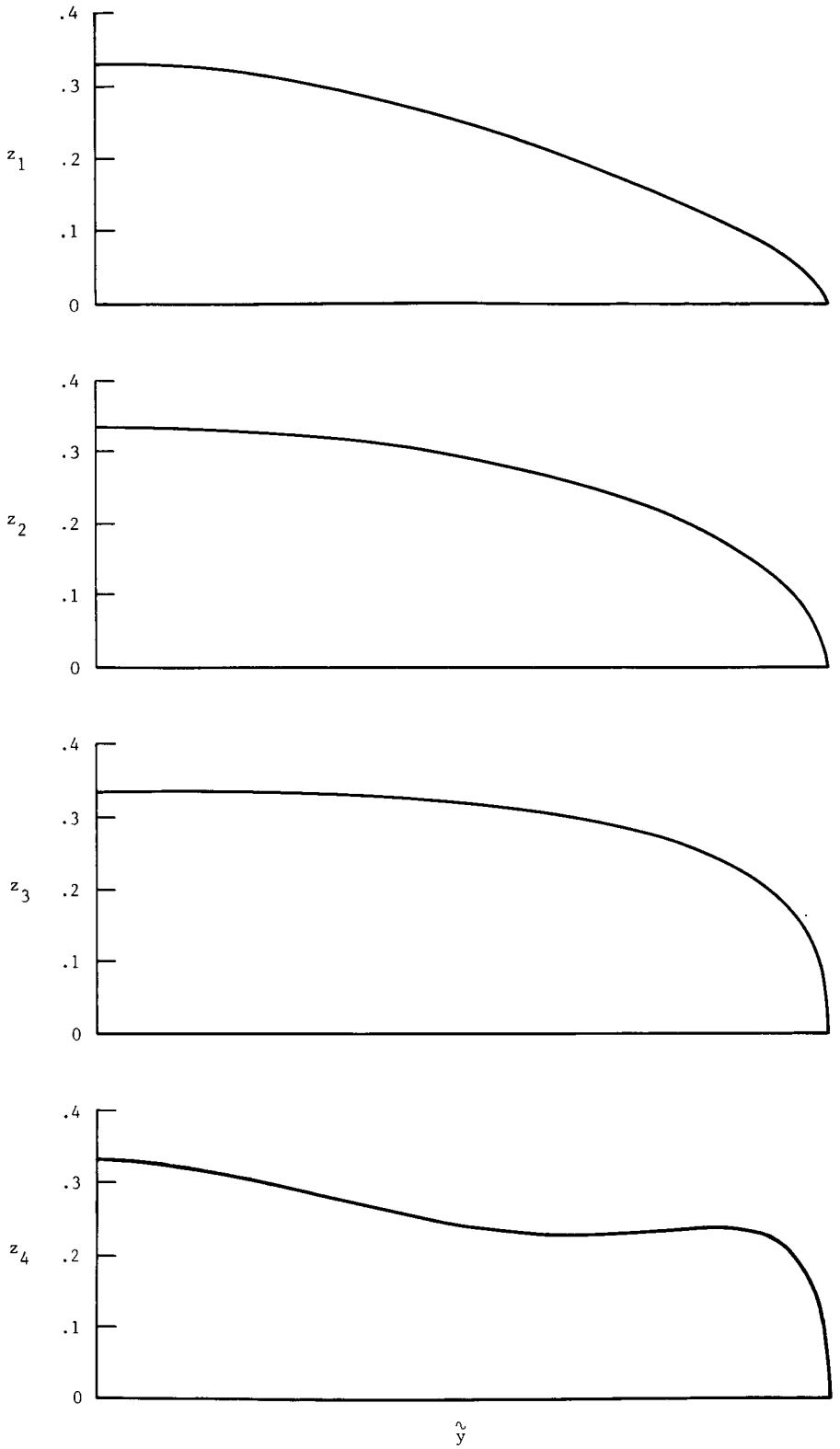

(a) Data base body cross-section shapes.

Figure 1. Model problem: Spanwise pressure design as function of body cross-section shape with $M = 1.4$, $\alpha = 5°$, Body length = 10 units, planform defined by $y = 0.5x(1 - x)$, and pressure specified at $x = 7.5$.

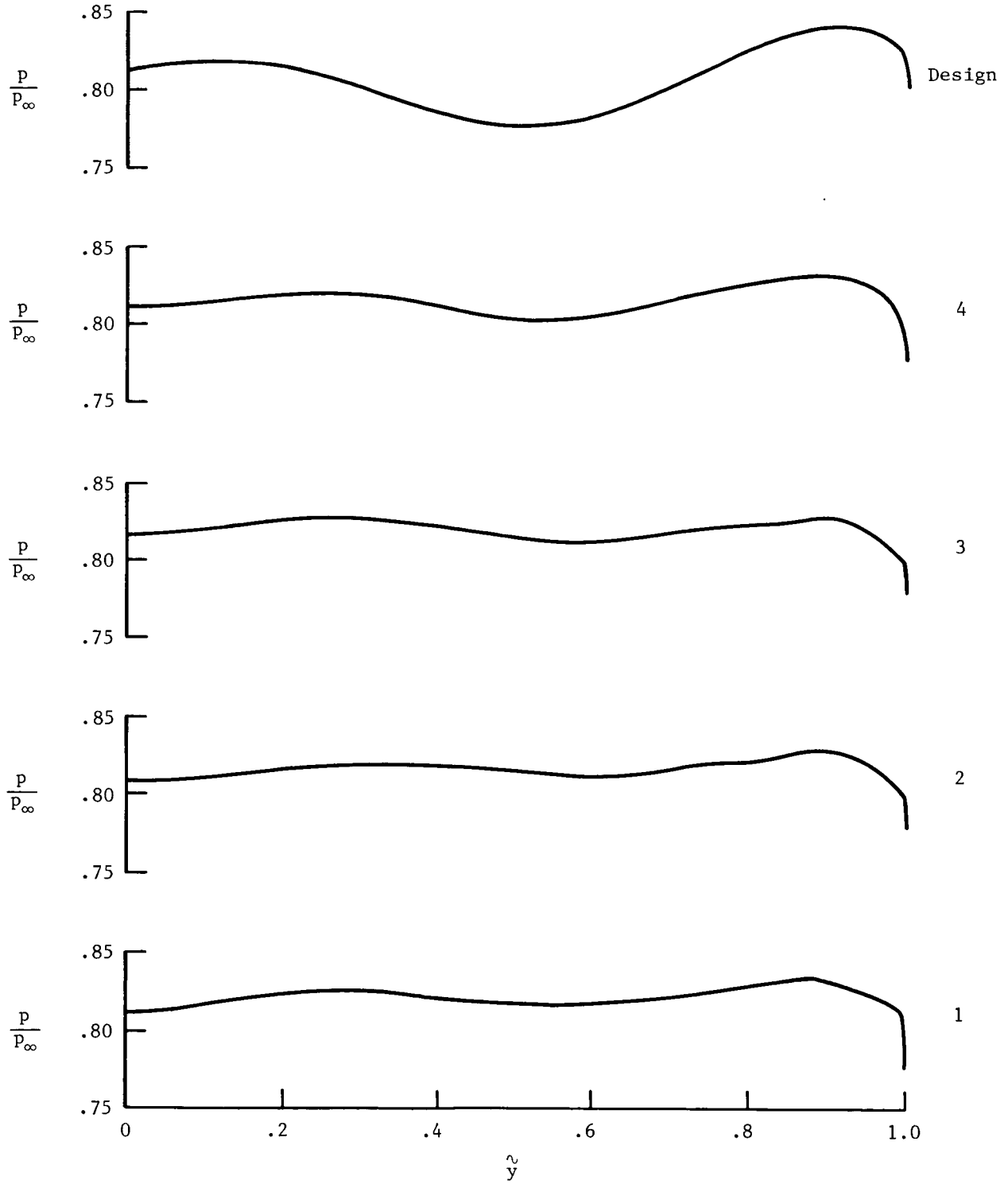

(b) Data base pressure and design pressure distribution.

Figure 1. Continued.

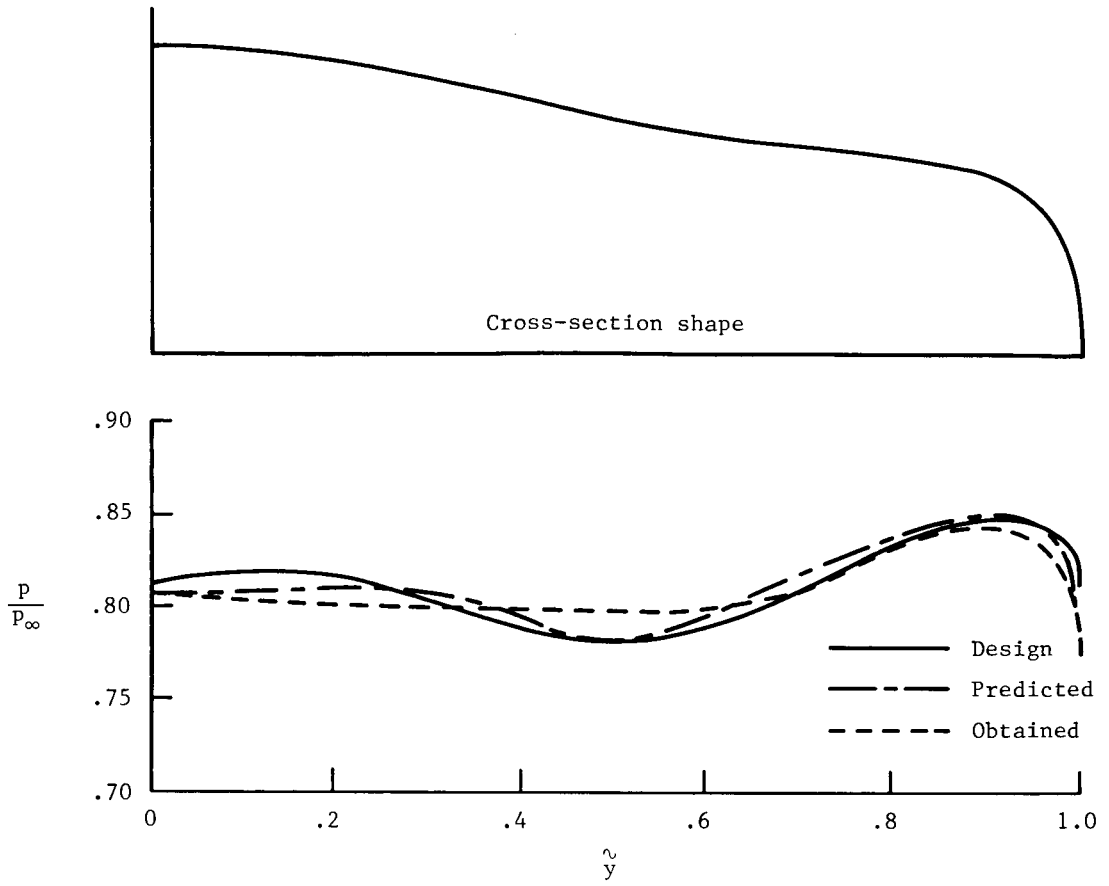

(c) Comparison of optimum combination predicted and computed pressures with design pressure and corresponding body cross-section shape.

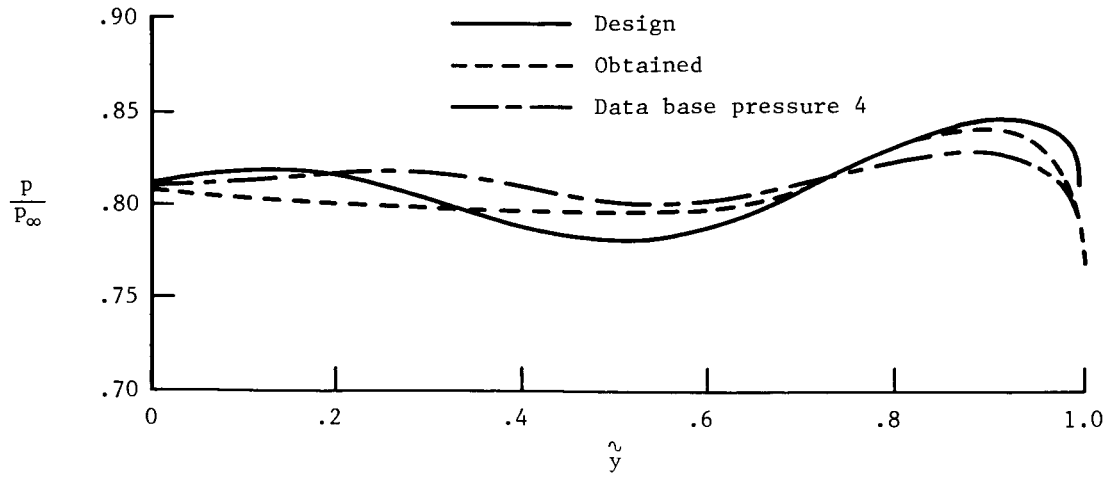

(d) Comparison of nearest approximation data base pressure and optimum combination pressure with design pressure distribution.

Figure 1. Concluded.

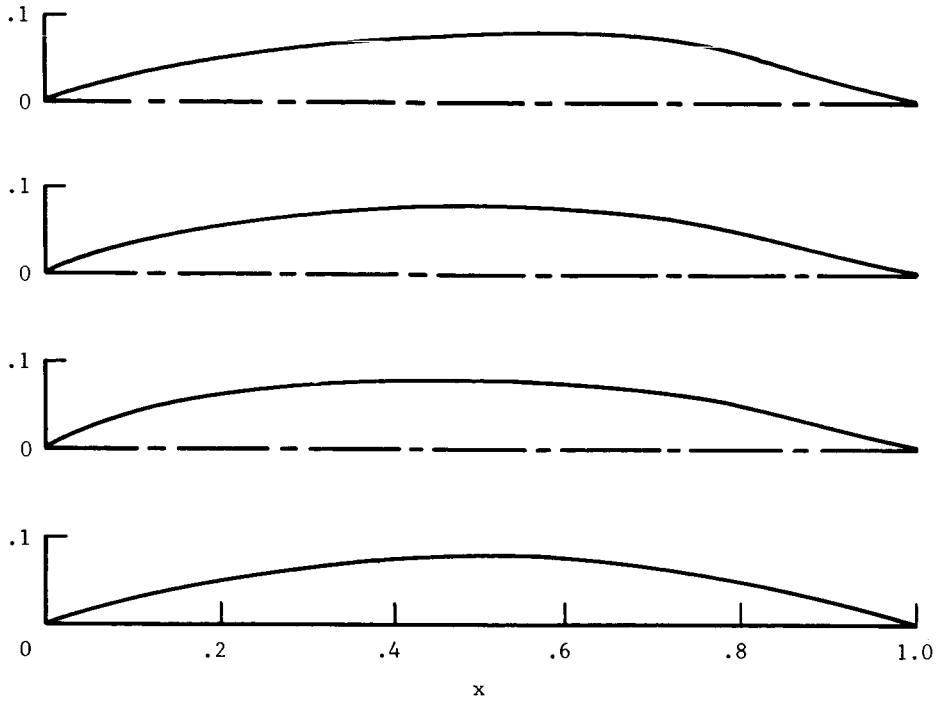

(a) Data base body shapes.

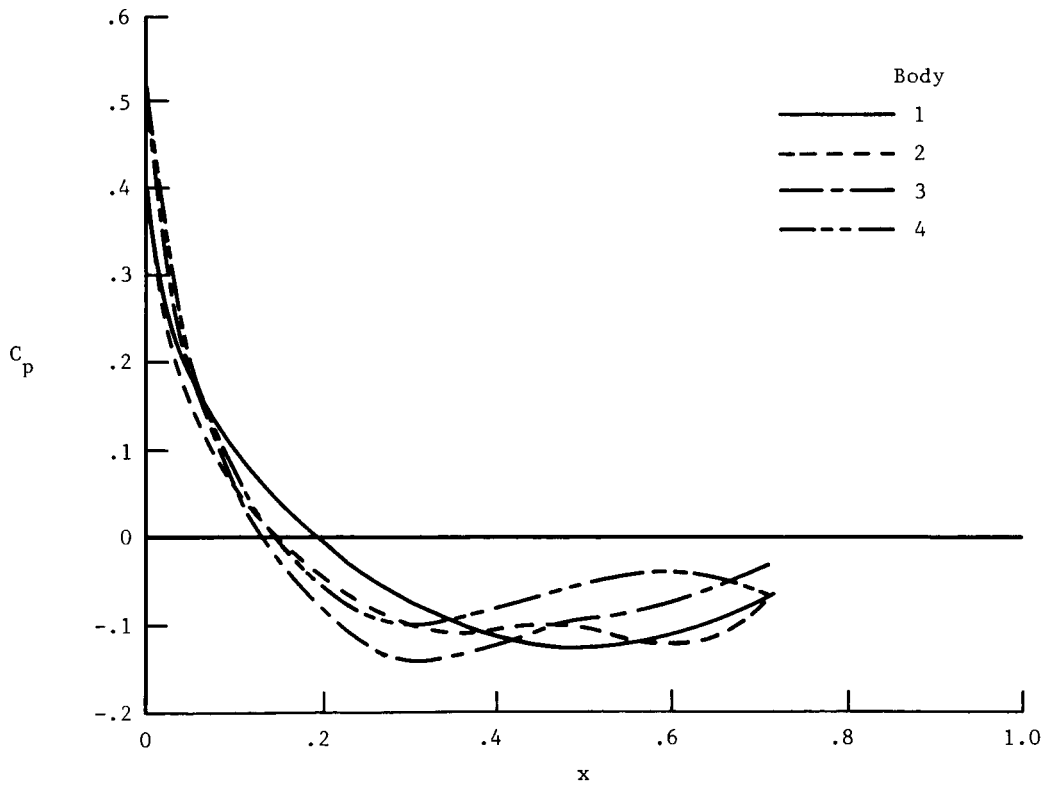

(b) Data base pressure distributions.

Figure 2. Model problem: Pressure distribution design on forward 60 percent of low-speed axisymmetric body.

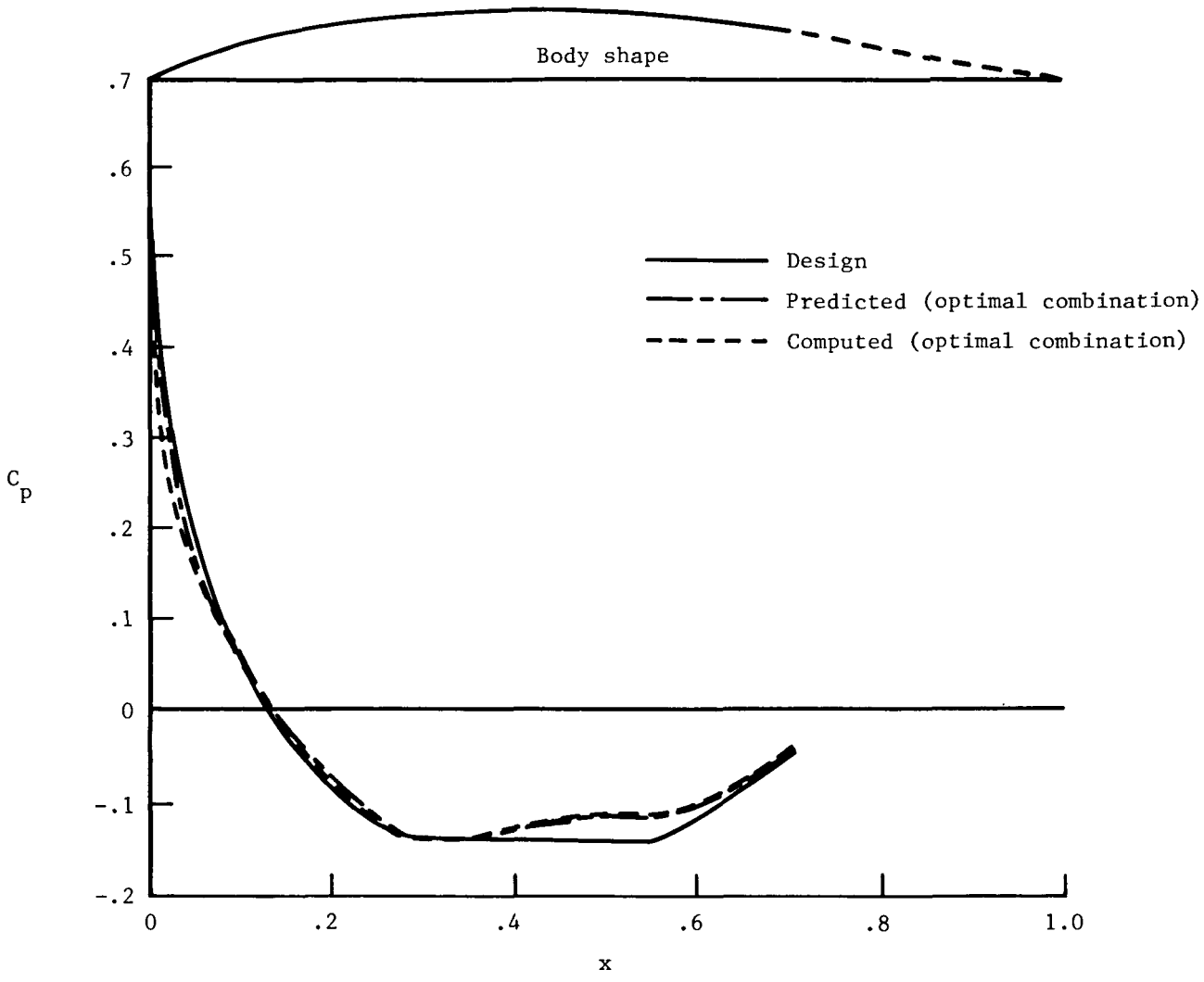

(c) Comparison of optimum combination predicted and computed pressures and design pressure distribution with corresponding body shape.

Figure 2. Concluded.

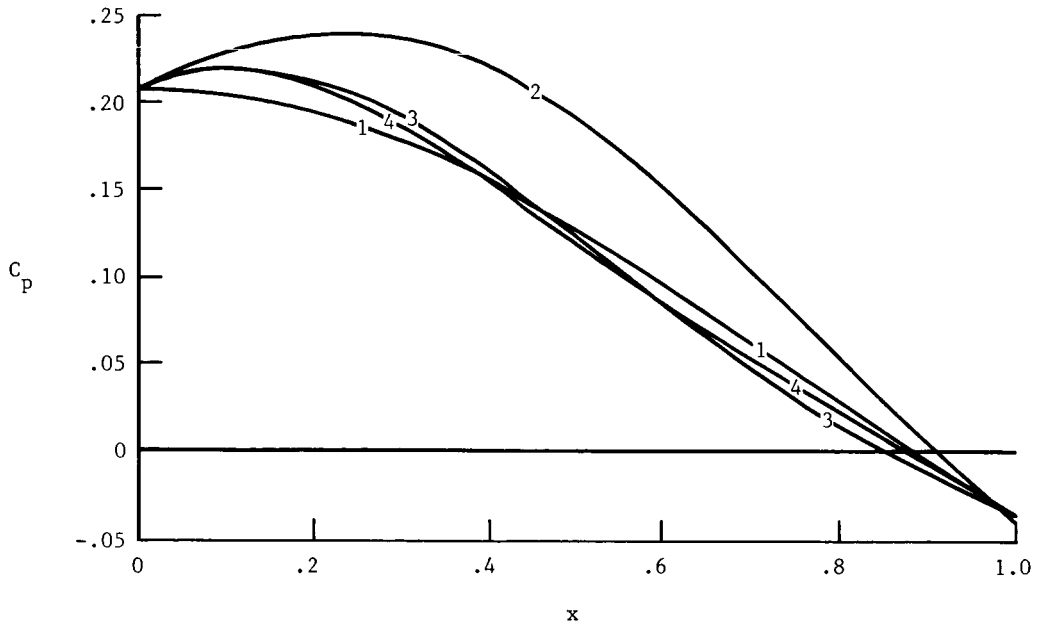

(a) Data base pressures.

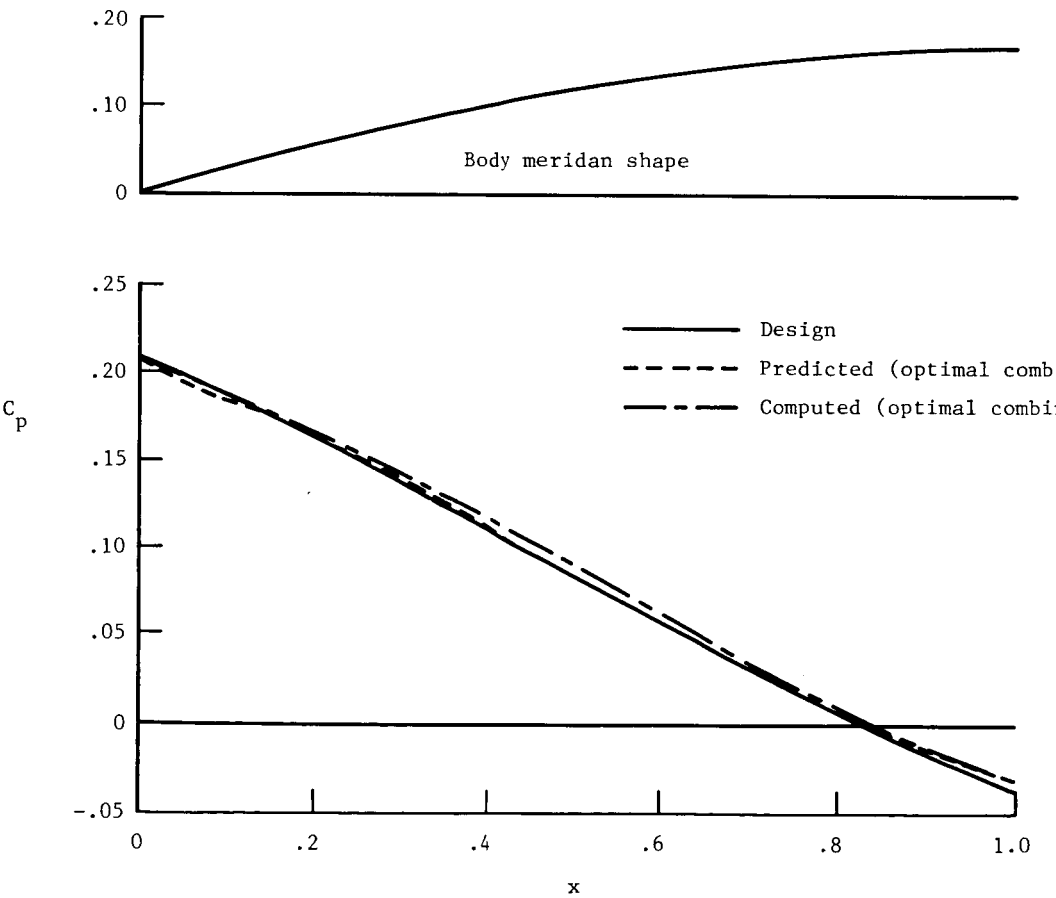

(b) Optimum combination predicted and computed pressures, design pressure, and optimum combination shape.

Figure 3. Model problem: Pressure design for Mach 3.0 axisymmetric forebody.

NASA
National Aeronautics and Space Administration

Report Documentation Page

1. Report No.	2. Government Accession No.	3. Recipient's Catalog No.
NASA TP-2706		

4. Title and Subtitle	5. Report Date
On Minimizing the Number of Calculations in Design-by-Analysis Codes	June 1987
	6. Performing Organization Code
7. Author(s)	8. Performing Organization Report No.
Raymond L. Barger and Anutosh Moitra	L-16226
9. Performing Organization Name and Address	10. Work Unit No.
NASA Langley Research Center Hampton, VA 23665-5225	505-68-91-09
	11. Contract or Grant No.
12. Sponsoring Agency Name and Address	13. Type of Report and Period Covered
National Aeronautics and Space Administration Washington, DC 20546-0001	Technical Paper
	14. Sponsoring Agency Code

15. Supplementary Notes

Raymond L. Barger: Langley Research Center, Hampton, Virginia.
Anutosh Moitra: High Technology Corporation, Hampton, Virginia.

16. Abstract

A method has been presented for aerodynamic design for a specified pressure distribution, using analysis codes only. The method requires a very conservative number of analysis runs, and therefore is appropriate when the analysis code is a large code in terms of storage and/or running time. Three model problems illustrate some capabilities and limitations of the method.

17. Key Words (Suggested by Authors(s))	18. Distribution Statement
Design Optimal design Aerodynamic design	Unclassified—Unlimited Subject Category 02

19. Security Classif.(of this report)	20. Security Classif.(of this page)	21. No. of Pages	22. Price
Unclassified	Unclassified	14	A02

For sale by the National Technical Information Service, Springfield, Virginia 22161-2171